Project 2

Overview

This project implemented the Crank-Nicolson(CN) scheme and Alternating-direction implicit (ADI) method to solve the 1D and 2D time-dependent Schrödinger equation. The order of accuracy of these two schemes was verified by 4-level convergence tests and I explored the scattering behavior of a quantum particle under different potential conditions.

Problem 1

Introduction

The non-dimensionalized 1D Schrödinger equation is solved on unit space interval on $0 < t < t_{max}$:

$$i\psi(x,t)_t = -\psi_{xx} + V(x,t)\psi$$

$$\psi(x,0) = \psi_0(x)$$

$$\psi(0,t) = \psi(1,t) = 0$$

The initial data ψ_0 can be either of exact family:

$$\psi(x,0) = sin(m)$$

or boosted Gaussian:

$$\psi(x,0) = e^{ipx}e^{-((x-x_0)/\sigma)^2}$$

The time-independent potential takes a certain value V_c over some interval of x if there is a potential barrier/well and is zero everywhere else. The "running integral" of the probability density is introduced as a diagnostic statistic, defined as:

$$P(x,t) = \int_0^x \psi(\tilde{x},t)\psi^\star(\tilde{x},t)d\tilde{x}$$

Implementation

The C-N scheme for 1D Schrödinger equation can be written in the following form:

$$c_j^-\psi_{j-1}^{n+1} + c_j^0\psi_j^{n+1} + c_j^+\psi_{j+1}^{n+1} = b_j^-\psi_{j-1}^n + b_j^0\psi_j^n + b_j^+\psi_{j+1}^n$$

$$c_j^- = c_j^+ = \frac{1}{2\Delta x^2}$$

$$c_j^0 = \frac{i}{\Delta t} - \frac{1}{\Delta x^2} - \frac{1}{2}V_j^{n+\frac{1}{2}}$$

$$b_j^- = b_j^+ = -\frac{1}{2\Delta x^2}$$

$$b_j^0 = \frac{i}{\Delta t} + \frac{1}{\Delta x^2} + \frac{1}{2}V_j^{n+\frac{1}{2}}$$

Because ψ_{j-1}^n, ψ_j^n, and ψ_{j+1}^n are known values, the right hand side as a function of ψ^n can be directly calculated through the following matrix multiplication:

$$f(\psi^n) = B\psi^n$$

$$B = \begin{bmatrix} b_1^0 & b_1^+ & \cdot & \cdot & \cdot & \cdot & \cdot \\ b_2^- & b_2^0 & b_2^+ & \cdot & \cdot & \cdot & \cdot \\ \cdot & \star & \star & \star & \cdot & \cdot & \cdot \\ \cdot & \cdot & \star & \star & \star & \cdot & \cdot \\ \cdot & \cdot & \cdot & \cdot & b_{j-1}^- & b_{j-1}^0 & b_{j-1}^+ \\ \cdot & \cdot & \cdot & \cdot & \cdot & b_j^- & b_j^0 \end{bmatrix}$$

where $b_1^0 = b_j^0 = 1, b_1^+ = b_j^- = 0$ to satisfy the boundary conditions. Similarly, the advanced unknowns can be solved by setting up the tridiagonal system:

$$A\psi^{n+1} = f(\psi^n) \tag{1}$$

$$A = \begin{bmatrix} c_1^0 & c_1^+ & \cdot & \cdot & \cdot & \cdot & \cdot \\ c_2^- & c_2^0 & c_2^+ & \cdot & \cdot & \cdot & \cdot \\ \cdot & \star & \star & \star & \cdot & \cdot & \cdot \\ \cdot & \cdot & \star & \star & \star & \cdot & \cdot \\ \cdot & \cdot & \cdot & \cdot & c_{j-1}^- & c_{j-1}^0 & c_{j-1}^+ \\ \cdot & \cdot & \cdot & \cdot & \cdot & c_j^- & c_j^0 \end{bmatrix}$$

$$c_1^0 = c_j^0 = 1$$

$$c_1^+ = c_j^- = 0$$

Both A and B are stored as a sparse matrix by passing the three diagonals to `spdiags`. At each time step, the RHS in equation (1) is calculated using the solution from the previous time step, and ψ^{n+1} is solved by left division.

After solving the equation on the entire domain, the running integral $P(x,t)$ is calculated using trapezoidal approximation. The probability density $|\psi|^2$ is passed to `cumtrapz` to calculate the cumulative integral along the x dimension, such that the result is a $nt \times nx$ array.

Convergence Test

4-level convergence tests were conducted from the solution of exact family and boosted Gaussian. For levels 6, 7, 8, $||d\psi^l||_2(t^n)$ was plotted against time, where

$$||d\psi^l||_2(t^n) = RMS(\psi^{l+1}(t^n) - \psi^l(t^n))$$

For solutions of the exact family, an additional test was performed on the absolute difference $||E\psi^l||_2(t^n)$ between the CN solution and the exact solution:

$$||E\psi^l||_2(t^n) = RMS(\psi^l(t^n) - \psi_{exact}(t^n))$$

$$\psi_{exact}(x,t) = e^{-3^2 i\pi^2 t} sin(3\pi x) \tag{2}$$

The exact solution (2) was calculated for every grid point on the x-t meshgrid used in the CN scheme. The RMS was then taken along the t dimension of the difference matrix to get the error at each time step. Figure 1 - 3 show the results of the three convergence tests.

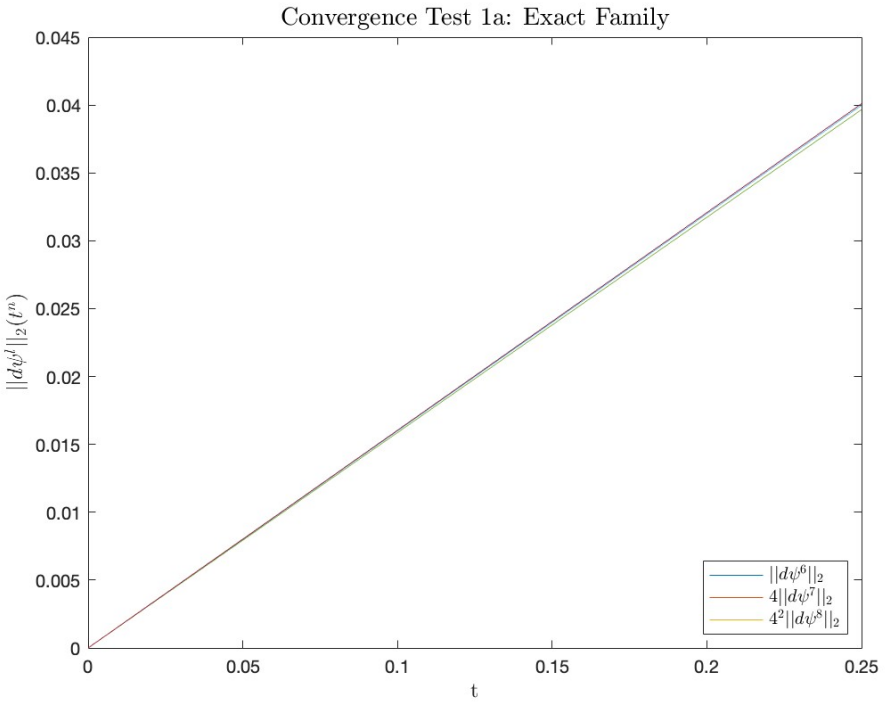

Figure 1: Scaled level-to-level error plot of exact family solution

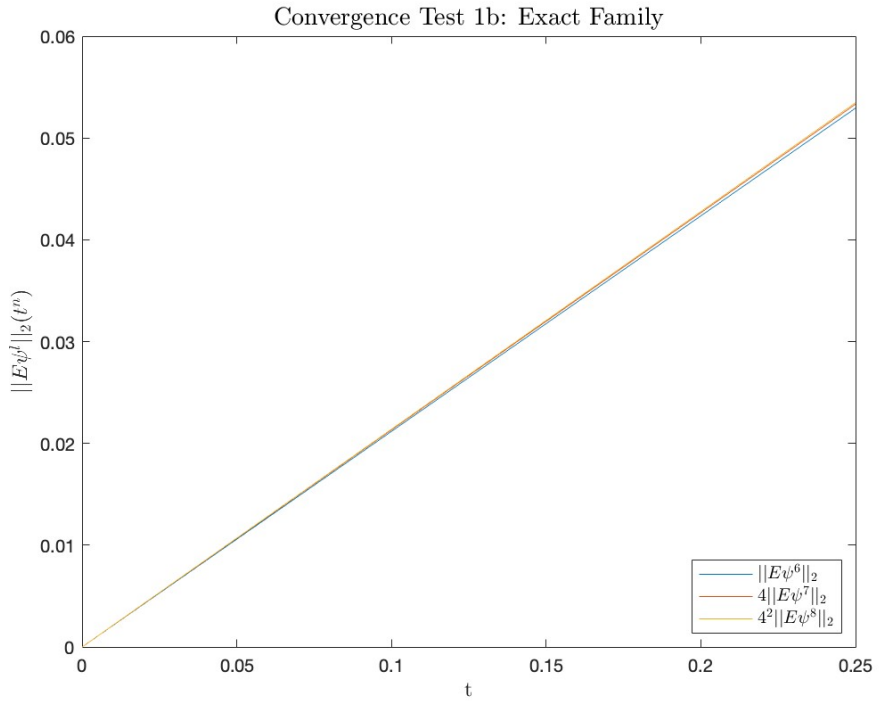

Figure 2: Scaled exact error plot of exact family solution

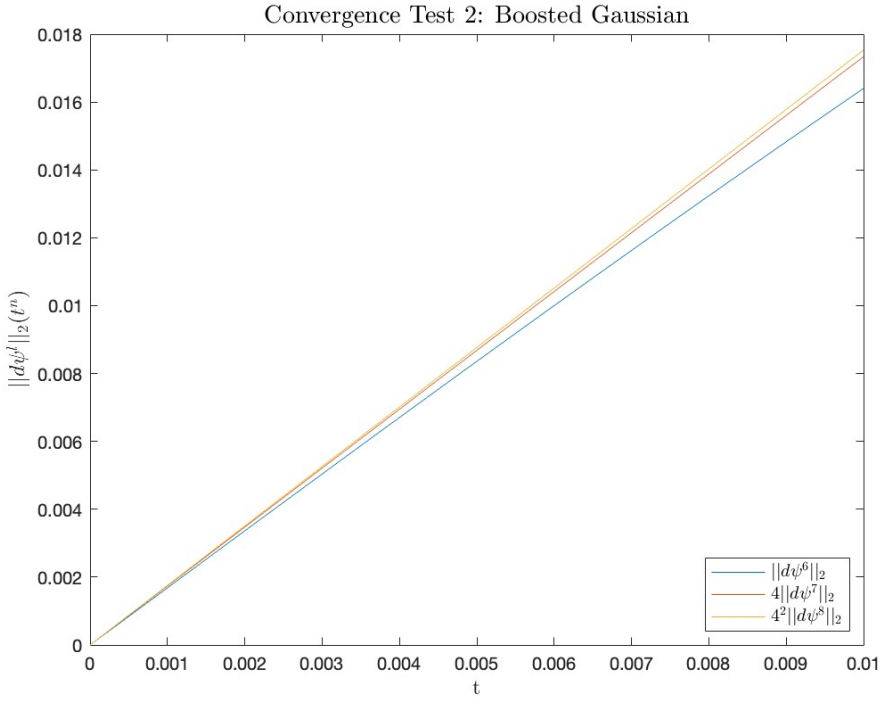

Figure 3: Scaled level-to-level error plot of boosted Gaussian solution

In each convergence test, errors in levels 7 and 8 were scaled by 4 and 4^2 respectively. After scaling, the three curves show near coincidence. This implies that the solution gets more accurate by 4 times as

the grid gets finer by half. So the method is second-order accurate in Δx and Δt.

Barrier/Well Survey

Define $\bar{P}_j$ as the temporal average of the discrete running integrals at x_j, and assume that all temporal averages are normalized by $\bar{P}_{n_x}$ such that $\bar{P}_{n_x} = 1$. $\bar{P}_{x_2} - \bar{P}_{x_1}$ can be interpreted as the fraction of time that the quantum particle spends in the interval $x_2 - x_1$. Since the Schrodinger equation is solved on the unit interval, a free particle is expected to have $\bar{P}(x_2) - \bar{P}(x_1) \to x_2 - x_1$ at sufficiently large times. If a potential barrier/well is included, $\bar{P}(x_2) - \bar{P}(x_1)$ should change under different potential conditions. The excess fractional probability is the ratio of how long the particle spends in the $x_2 - x_1$ interval compared to how long a free particle would.

$$\bar{F}_e(x_1, x_2) = \frac{\bar{P}(x_2) - \bar{P}(x_1)}{x_2 - x_1}$$

In the following surveys, $ln(\bar{F}_e(x_1, x_2))$ was plotted against $ln(V_0)$, where V_0 is the height of the potential barrier or the depth of the potential well.

- Barrier Survey

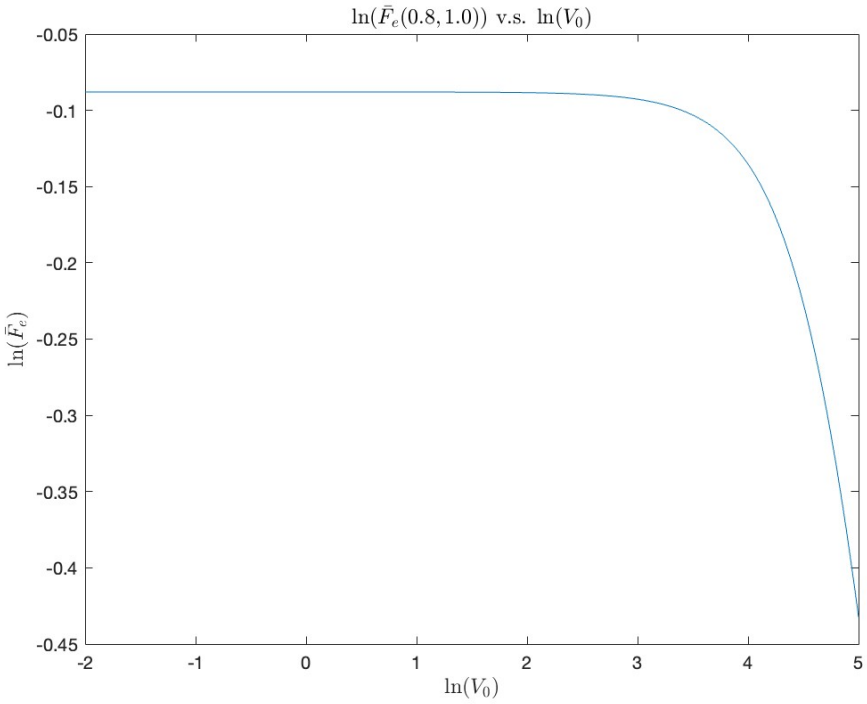

Figure 4: Excess fractional probability to the right of the barrier for $V_0 \in [e^{-2}, e^5]$

From the graph we can see that $ln(\bar{F}_e)$ is negative for all barriers, which means the particle is less likely to be found to the right of the barrier when a potential is present. Larger $ln(V_0)$ means increasingly high potential walls, so the particle becomes less likely to tunnel through the barrier.

- Well Survey

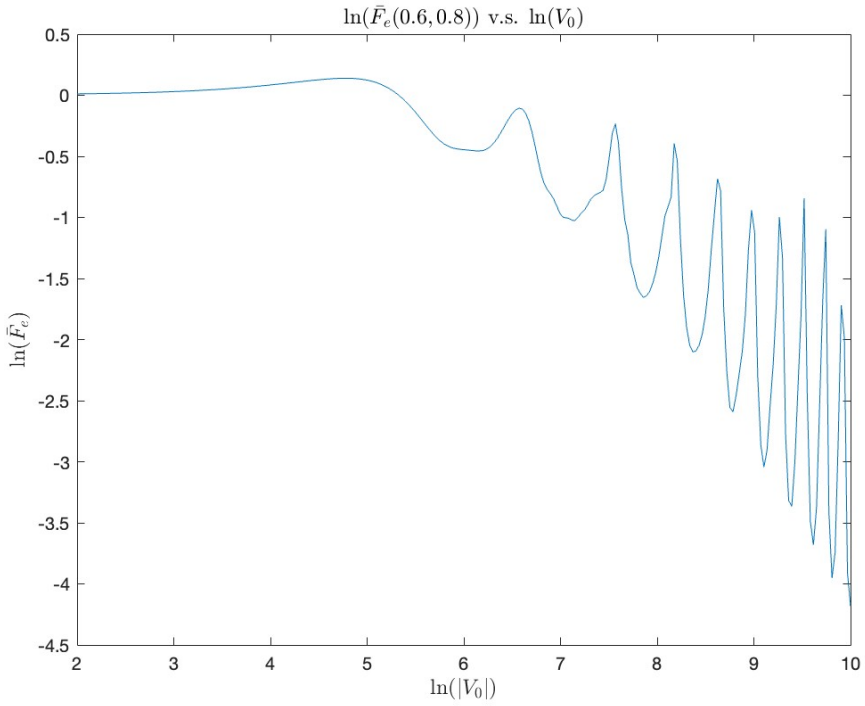

Figure 5: Excess fractional probability in the well for $V_0 \in [-e^2, e^{10}]$

When the well is shallow, $ln(F_e) > 0$ which means the particle lingers in the well longer than a free particle does. After the point where $|V_0| > e^5$, as V_0 becomes more negative, the particle generally spends less time in the well , and shows increasingly obvious fluctuations. In the bound region of a potential well, only solutions at certain discrete energy levels are allowed. The spikes get closer together as the potential increases, which corresponds to the different quantized energy levels of the system.

Problem 2

Introduction

In this problem we solve the following 2D Shrödinger equation:

$$\psi(x, y, t)_t = i(\psi_{xx} + \psi_{yy}) - iV(x, y)\psi$$

$$\psi(x, y, 0) = \psi_0(x, y)$$

$$\psi(0, y, t) = \psi(1, y, t) = \psi(x, 0, t) = (x, 1, t) = 0$$

The domain for this problem is

$$0 \leq x \leq 1, \qquad 0 \leq y \leq 1, \qquad 0 \leq t \leq t_{max}$$

The continuum domain is discretized with level l and the ratio of temporal to spatial mesh spacins λ:

$$\Delta x = \Delta y = 2^{-l}$$

$$\Delta t = \Delta x$$

Three types of potentials are considered:

- No potential: V is zero on entire domain.
- Rectangular barrier or well: V takes some specified positive/negative value on one rectangular space domain.
- Double slit: V forms a narrow barrier at $y = 0.25$. Two openings are specified by their x coordinates.

Analogous to the 1D equation, the initial data can be either of exact family or boosted Gaussian.

Implementation

The ADI discretization used is:

$$\left(1 - i\frac{\Delta t}{2}\delta^h_{xx}\right)\psi^{n+\frac{1}{2}}_{i,j} = \left(1 + i\frac{\Delta t}{2}\delta^h_{xx}\right)\left(1 + i\frac{\Delta t}{2}\delta^h_{yy} - i\frac{\Delta t}{2}V_{i,j}\right)\psi^n_{i,j} \tag{3}$$

$$\left(1 - i\frac{\Delta t}{2}\delta^h_{yy} + i\frac{\Delta t}{2}V_{i,j}\right)\psi^{n+1}_{i,j} = \psi^{n+\frac{1}{2}}_{i,j} \tag{4}$$

The difference operators δ^h_{xx} and δ^h_{yy} are:

$$\delta^h_{xx} = \frac{u^n_{i+1,j} - 2u^n_{i,j} + u^n_{i-1,j}}{\Delta x^2}$$

$$\delta^h_{yy} = \frac{u^n_{i,j+1} - 2u^n_{i,j} + u^n_{i,j-1}}{\Delta y^2}$$

The initial data is assigned to the first page of the ψ 3D array. Equations (3) and (4) are solved sequentially in two stages at every time step.

Stage I

The RHS of (3) $f(\psi^n_{i,j})$ is calculated in two steps:

$$u^n_{i,j} = \left(1 + i\frac{\Delta t}{2}\delta^h_{yy} - i\frac{\Delta t}{2}V_{i,j}\right)\psi^n_{i,j} \tag{5}$$

$$f(\psi^n_{i,j}) = \left(1 + i\frac{\Delta t}{2}\delta^h_{xx}\right)u^n_{i,j} \tag{6}$$

Expand the difference operators in (5) and (6):

$$u_{i,j}^n = \left(\frac{i\Delta t}{2\Delta y^2}\right)\psi_{i,j-1}^n + \left(1 - \frac{i\Delta t}{\Delta y^2} - \frac{i\Delta t}{2}V_{i,j}\right)\psi_j^n + \left(\frac{i\Delta t}{2\Delta y^2}\right)\psi_{i,j+1}^n \tag{7}$$

$$f(\psi_{i,j}^n) = \left(\frac{i\Delta t}{2\Delta x^2}\right)u_{i,j-1}^n + \left(1 - \frac{i\Delta t}{\Delta x^2}\right)u_j^n + \left(\frac{i\Delta t}{2\Delta x^2}\right)u_{i,j+1}^n \tag{8}$$

$u_{i,j}^n$ is calculated by applying (7) to every row of $\psi_{i,j}^n$ except for the first and last row to sustain the boundary conditions. Every iteration uses the ith row of the potential matrix V. RHS of $f(\psi_{i,j}^n)$ doesn't have potential dependence, which means the operation is the same for every column. Therefore it is calculated using matrix multiplication directly:

$$f(\psi^n) = A_{RHS}(u^n)$$

$$A_{RHS} = \begin{bmatrix} a^0 & a^+ & \cdot & \cdot & \cdot & \cdot & \cdot \\ a^- & a^0 & a^+ & \cdot & \cdot & \cdot & \cdot \\ \cdot & \star & \star & \star & \cdot & \cdot & \cdot \\ \cdot & \cdot & \star & \star & \star & \cdot & \cdot \\ \cdot & \cdot & \cdot & \cdot & a^- & a^0 & a^+ \\ \cdot & \cdot & \cdot & \cdot & \cdot & a^- & a^0 \end{bmatrix}$$

$$a^- = a^+ = \frac{i\Delta t}{2\Delta x^2} \qquad a^0 = 1 - \frac{i\Delta t}{\Delta x^2}$$

The LHS of (3) can be written as:

$$\left(-\frac{i\Delta t}{2\Delta x^2}\right)\psi_{i-1,j}^{n+\frac{1}{2}} + \left(1 + \frac{i\Delta t}{\Delta x^2}\right)\psi_{i,j}^{n+\frac{1}{2}} + \left(-\frac{i\Delta t}{2\Delta x^2}\right)\psi_{i+1,j}^{n+\frac{1}{2}} \tag{9}$$

The operation on $\psi^{n+\frac{1}{2}}$ in (9) is set up as a tridiagonal sparse matrix A that has a similar structure to A_{RHS}. A satisfies the boundary conditions:

$$a_1^0 = a_j^0 = 1 \qquad a_1^+ = a_j^- = 0$$

The temporary array $\psi^{n+\frac{1}{2}}$ is then calculated by solving the system:

$$A\psi_j^{n+\frac{1}{2}} = f(\psi_j^n)$$

This system is supposed to be solved for every column of $\psi^{n+\frac{1}{2}}$, but since A is the same for every system and the jth column in $\psi^{n+\frac{1}{2}}$ corresponds to the jth column in $f(\psi^n)$, $\psi^{n+\frac{1}{2}}$ can be solved directly as an $nx \times ny$ matrix using left division:

$$A\psi^{n+\frac{1}{2}} = f(\psi^n)$$

Stage II

The LHS of (4) can be written as:

$$\left(-\frac{i\Delta t}{2\Delta y^2}\right)\psi_{i,j-1}^{n+1}+\left(1+\frac{i\Delta t}{\Delta y^2}+\frac{i\Delta t}{2}V_{i,j}\right)\psi_{i,j}^{n+1}+\left(-\frac{i\Delta t}{2\Delta y^2}\right)\psi_{i,j+1}^{n+1} \tag{10}$$

A tridiagonal sparse matrix B satisfying (10) is set up for every row of ψ^{n+1} such that:

$$B_i\psi_i^{n+1}=\psi_i^{n+\frac{1}{2}}$$

B satisfies the same boundary conditions as A. The loop of solving the above system goes over $x_i = 2 : nx$ and in each iteration, B uses the ith row in the potential matrix. The final solution is output as an $nt \times nx \times ny$ 3D array.

Convergence Test

The convergence test was performed in `ctest_2d` for the following exact family solution with no potential applied:

$$\psi(x,y) = sin(2\pi x)sin(3\pi y)$$

The strategy is exactly the same as in Problem 1. The RMS value is calculated in both x and y dimensions because the difference between levels are 3D arrays. Figure 6 and Figure 7 show the level-to-level errors and actual errors over time.

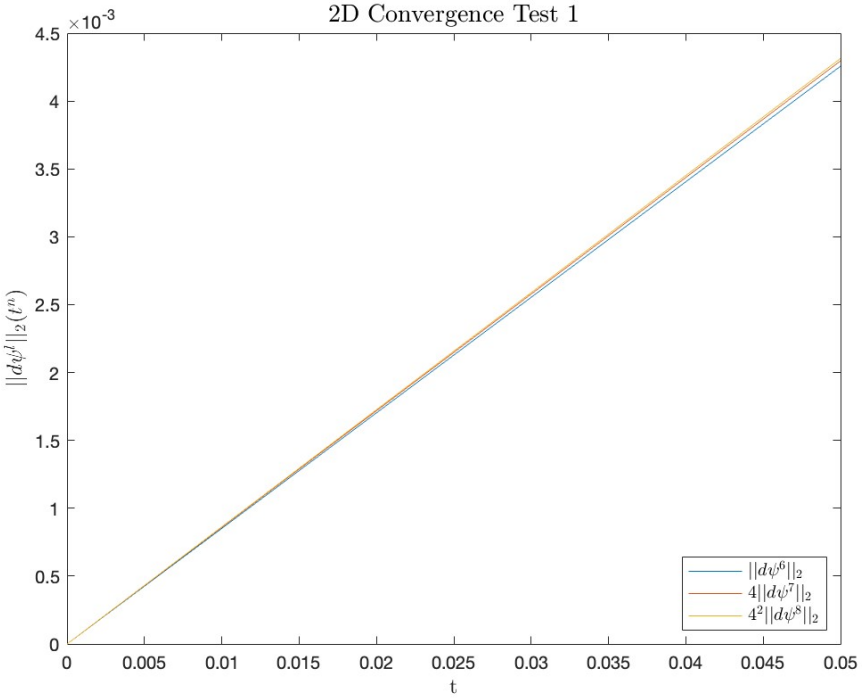

Figure 6: Scaled level-to-level error plot

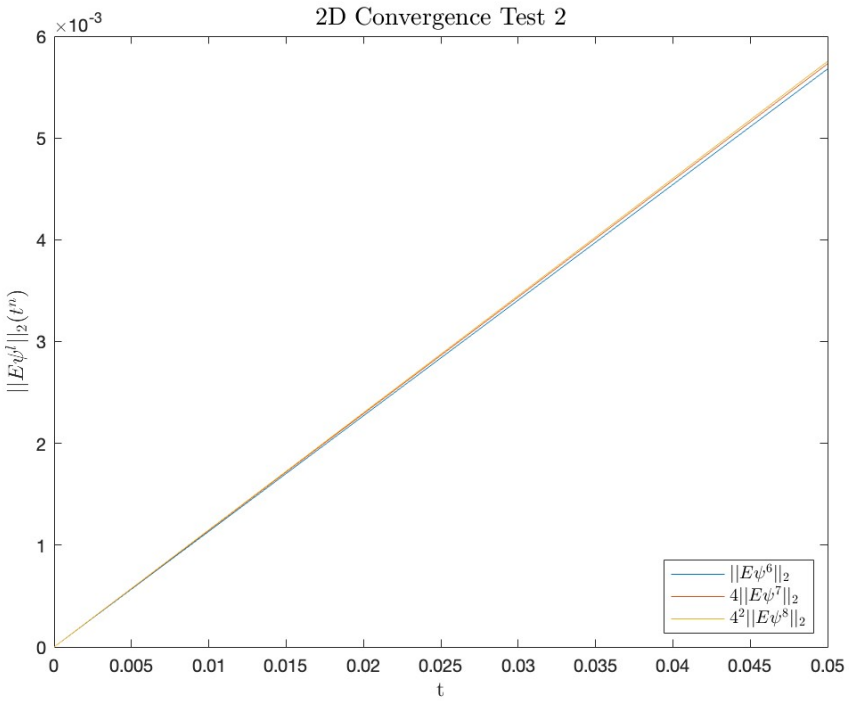

Figure 7: Scaled actual error plot

The actual errors from the exact solutions are slightly larger than the level-to-level errors, but in both plots the three error curves coincide after proper scaling of $\rho = 2$. This verifies that the ADI scheme used for 2D solve is also second-order accurate in Δx, Δy and Δt.

Scattering experiment

The implementation was used to conduct several experiments to explore quantum particle scattering. `contourf` was used to visualize the time-evolution of $|\psi|$ on the x-y plane. The following movies are generated in `scatter_barrier.m`, `scatter_well.m`, and `scatter_slit.m`.

- **Scattering off a rectangular barrier** `barrier.mp4`
  In this experiment, a rectangular barrier is set in the middle of the x-y space domain. The particle starts from the left of the screen and scatters off as it encounters the barrier. The potential of the barrier is set to be very high, so there is no visible presence of the particle inside the barrier region.

- **Scattering off a rectangular well**: `well.mp4`
  In this experiment, a rectangular well is set in the middle of the x-y space domain. The particle starts from the left of the screen and scatters off as it encounters the well. The behaviour of the particle inside the well is different from when it's outside. The packets are significantly smaller and more discrete. It corresponds to the fact the the particles can only be found at certain positions in the well.

- **Double-slit**: `double_slit.mp4`
  In the double-slit experiment, the particle starts from the left of the barrier and scatters through

the two slits. The patterns created by self-interference can be clearly seen in the center of the screen after some time. The alternating dark and bright fringes are results from this self-interference.

- **Single-slit**: `single_slit.mp4`
  The same initial data as in the double-slit experiment is used here but the particle only scatters through a single slit. The wave-like behavior is also obvious after the scattering.

In all four experiments, the initial data is of the boosted Gaussian type with a boost in the horizontal direction. For the barrier/well experiment, the particle is relatively round with no obvious skewing in either direction. For the slit scattering experiments, the particle is made in a cigar shape that is flat in the x direction, so that the wave-like behavior is more pronounced through the slits.